Fitoterapia 142 (2020) 104491

Contents lists available at ScienceDirect

Fitoterapia

journal homepage: www.elsevier.com/locate/fitote

# Bousangine A, a novel C-17-nor aspidosperma-type monoterpenoid indole alkaloid from *Bousigonia angustifolia*

Zong-Qing Huo[a,b], Qian Zhao[a], Jian-Wen Liu[a], Wen-Tao Zhu[a], Xiao-Jiang Hao[a,*], Yu Zhang[a,*]

[a] State Key Laboratory of Phytochemistry and Plant Resources in West China, Kunming Institute of Botany, Chinese Academy of Sciences, Kunming 650201, PR China
[b] University of Chinese Academy of Sciences, Beijing 100049, PR China

ARTICLE INFO

*Keywords:*
*Bousigonia angustifolia*
Monoterpenoid indole alkaloids
Bousangines A and B

ABSTRACT

Two new monoterpenoid indole alkaloids, bousangines A (**1**) and B (**2**), were isolated from the twigs and leaves of *Bousigonia angustifolia*. Their structures including absolute configurations were elucidated by a combination of MS, NMR, ECD calculation, and single-crystal X-ray diffraction analysis. Bousangine A (**1**) possessed a rearrangement pentacyclic skeleton derived from aspidosperma-type alkaloids with C-17 degradation. Their antiproliferative activity against several human cancer cell lines were evaluated.

## 1. Introduction

Apocynaceae is a big plant family producing structurally and biologically interesting monoterpenoid indole alkaloids (MIAs), such as reserpine, vinblastine, and catharanthine [1]. The genus *Bousigonia* belongs to the Apocynaceae family and is distributed mainly in China, Laos, and Vietnam, containing only two species [2]. To date, more than 100 alkaloids have been isolated from this genus, most of them belong to monoterpenoid indole alkaloids, mainly comprising aspidosperma, eburnea, and aspidosperma-eburnea type alkaloids [3–7]. Some of them showed significant cytotoxicity [3–5,7], and preventing high glucose-induced podocyte injury activity [6]. To search for more structurally interesting MIAs, the chemical constituents of the twigs and leaves of *Bousigonia angustifolia* were investigated, and two new MIAs, bousangines A (**1**) and B (**2**), along with 10 known ones, namely (+)-vincadifformine (**3**) [8], eburenine (**4**) [9], eburnamenine (**5**) [10], *O*-methyl-vincanol (**6**) [11], (−)-*O*-ethyleburnamine (**7**) [12], (−)-*O*-methyleburnamine (**8**) [12], (−)-eburnamine (**9**) [12], leuconicine D (**10**) [13], (−)-leuconolam (**11**) [14], and (+)-melohenine B (**12**) [15] were isolated and identified. Bousangine A (**1**) possessed a rearrangement pentacyclic skeleton derived from aspidosperma-type alkaloids with C-17 degradation. Herein, we report the isolation, structure elucidation and biological tests of these alkaloids.

## 2. Experimental

### 2.1. General experimental procedures

NMR spectra were measured via a Bruker AV-500 MHz, or a Bruker Avance III 600 MHz, TMS was used as an internal standard. IR spectra were surveyed on a Bio-Rad FTS-135 with KBr pellets. A JASCO P-1020 digital polarimeter was used to get optical rotations, while the ECD spectral data were measured by an Applied Photophysics Chariscan Spectrometer. HRESIMS and ESI were surveyed on Aglient 1290 UPLC/6540 Q-TOF spectrometer. Silica gel (80–100 and 100–200 mesh, Qingdao Marine Chemical Inc., China), silica gel H (10–40 μm, Qingdao Marine Chemical Inc., China), and Sephadex LH-20 (40–70 μm, Amersham Pharmacia Biotech AB), were used for column chromatography. Semi-preparative HPLC was carried out using a Shimadzu LC-20AT liquid chromatograph equipped with a YMC Triart C18 ExRS (5 μm; 10 × 250 mm) reversed-phase column.

### 2.2. Plant material

The twigs and leaves of *B. angustifolia* were collected in Xishuangbanna, Yunnan Province, People's Republic of China, in July 2018. The samples were identified by Mr. Yu Chen, Kunming Botanical Garden. A specimen (no. ZY20180723) was deposited at State Key Laboratory of Phytochemistry and Plant Resource in West China, Kunming Institute of Botany, Chinese Academy of Science (CAS).

* Corresponding authors.
*E-mail addresses:* haoxj@mail.kib.ac.cn (X.-J. Hao), zhangyu@mail.kib.ac.cn (Y. Zhang).

https://doi.org/10.1016/j.fitote.2020.104491
Received 2 January 2020; Received in revised form 1 February 2020; Accepted 1 February 2020
Available online 04 February 2020
0367-326X/ 

### 2.3. Extraction and isolation

The dried twigs and leaves of *B. angustifolia* (57 kg) were powdered and extracted three times with methanol. The extract was diluted with water and the pH was adjusted to 2–3 with hydrochloric acid (5%) and then extracted three times with petroleum ether. The water fraction was basified to pH 9–10 with sodium hydroxide (10%), then extracted with chloroform to get the crude alkaloids. The crude alkaloids (130 g) were separated on a silica gel column (100–200 mesh), and eluted with a gradient of chloroform-methanol (40:1 → 1:1) to yield 5 fractions (A-E). Fraction A (9.1 g) was purified by a RP-18 column (MeOH/$H_2O$, 50:50 → 100:0, *v*/v) to give four subfractions (AI-AIV). Subfraction AI (3.2 g) was purified by a RP-18 column (MeOH/$H_2O$, 50:50 → 100:0, *v*/v) and followed by semipreparative HPLC with MeOH/$H_2O$ (78:22, 1‰ v/v diethylamine) to give (+)-vincadifformine (**3**) (23.5 mg, $t_R$ 35.0 min). Subfraction AII (2.9 g) was purified by a RP-18 column (MeOH/$H_2O$, 50:50 → 100:0, *v*/v) and followed by semipreparative HPLC with MeOH/$H_2O$ (70:30, 1‰ v/v diethylamine) to afford eburenine (**4**) (14.7 mg, $t_R$ 27.5 min) and eburnamenine (**5**) (174.5 mg, $t_R$ 33.0 min). Subfraction AIII (1 g) was further separated by semipreparative HPLC with MeOH/$H_2O$ (60:40, 1‰ *v*/v diethylamine) to afford *O*-methyl-vincanol (**6**) (10.5 mg, $t_R$ 35.0 min). Fraction B (17.8 g) was purified by a RP-18 column (MeOH/$H_2O$, 30:70 → 100:0, *v*/v) to give two subfractions (BI-BII). Subfraction BI (8.2 g) was subjected to a silica gel chromatography column eluting with petroleum ether/acetone (50:1–2:1, *v*/v) and followed by semipreparative HPLC with MeOH/$H_2O$ (51:49, 1‰ v/v diethylamine) to give **1** (8.4 mg, $t_R$ 31.0 min), (−)-*O*-ethyleburnamine (**7**) (10.0 mg, $t_R$ 42.0 min) and (−)-*O*-methyleburnamine (**8**) (3.8 mg, $t_R$ 55.0 min). Subfraction BII (6.5 g) was subjected a silica gel chromatography column eluting with petroleum ether/acetone (35:1–2:1, *v*/v) and then by semipreparative HPLC with MeOH/$H_2O$ (55:45, 1‰ v/v diethylamine) to afford **2** (10.3 mg, $t_R$ 40.0 min), (−)-eburnamine (**9**) (8.0 mg, $t_R$ 47.0 min), and leuconicine D (**10**) (10.0 mg, $t_R$ 55.0 min). Fraction C (8.6 g) was purified by a RP-18 column (MeOH/$H_2O$, 30:70 → 100:0, *v*/v) to give three subfractions (CI-CIII). Subfraction CI (2.1 g) was subjected to a series of silica gel chromatography column eluting with petroleum ether/acetone (15:1–2:1, *v*/v) and followed by semipreparative HPLC with MeOH/$H_2O$ (86:14, 1‰ v/v diethylamine) to afford (−)-leuconolam (**11**) (5.1 mg, $t_R$ 45.0 min). Subfraction CII (3.5 g) was subjected to a silica gel chromatography column eluting with petroleum ether/acetone (12:1–1:1, *v*/v) and followed by semipreparative HPLC with MeOH/$H_2O$ (75:25, 1‰ v/v diethylamine) to give (+)-melohenine B (**12**) (7.3 mg, $t_R$ 30.0 min).

### 2.4. Bousangine a (1)

*Bousangine A (1):* white solid; [α]20 D + 20.7 (*c* 0.16, $CH_3OH$); UV ($CH_3OH$) $\lambda_{max}$ (log $\varepsilon$): 221 (3.99), 264 (3.57) nm; ECD (0.00095 M, $CH_3OH$) $\lambda_{max}$ ($\Delta\varepsilon$) 204 (−7.63), 274 (+5.95); IR (KBr) $\nu_{max}$ 3433, 2924, 1737, 1631, 1590, 1484, 1264, 1147 $cm^{-1}$; $^1H$ and $^{13}C$ NMR data (acetone–$d_6$, 500 and 125 MHz) see Table 1; HRESIMS *m/z* 339.1708 $[M + H]^+$ (calcd for $C_{20}H_{22}N_2O_3$, 339.1703).

### 2.5. Bousangine B (2)

*Bousangine B (2):* colorless solid; [α]20 D − 36.2 (*c* 0.11, $CH_3OH$); UV ($CH_3OH$) $\lambda_{max}$ (log $\varepsilon$): 229 (3.01), nm; ECD (0.00066 M, $CH_3OH$) $\lambda_{max}$ ($\Delta\varepsilon$) 199 (+2.30), 230 (−3.20), 321 (+0.65); IR (KBr) $\nu_{max}$ 3439, 2920, 1735, 1683, 1632, 1466, 1350, 1218, 1059 $cm^{-1}$; $^1H$ and $^{13}C$ NMR data (acetone–$d_6$, 500 and 125 MHz) see Table 1; HRESIMS *m/z* 365.1846 $[M + Na]^+$ (calcd for $C_{20}H_{26}N_2O_3$, 365.1836).

### 2.6. Cytotoxicity assays

Cytotoxicity evaluations were performed according to the previously described protocol [5].

**Table 1**
$^1H$ NMR Data of Bousangines A and B (**1** and **2**).

| No. | 1 | | 2 | |
|---|---|---|---|---|
| | $\delta_H$[a] | $\delta_C$[b] | $\delta_H$[a] | $\delta_C$[b] |
| 2 | | 182.2 | | 172.9 |
| 3a | 3.04 (1H, ddd, 14.0, 11.5, 4.5) | 44.3 | 2.41 (1H, ddd, 12.5, 11.0, 3.0) | 57.1 |
| 3b | 3.10 (1H, m) | | 2.94 (1H, m) | |
| 5a | 3.21 (1H, ddd, 12.0, 9.5, 3.0) | 47.2 | 2.90 (1H, m) | 53.5 |
| 5b | 3.32 (1H, m)[c] | | 2.91 (1H, m) | |
| 6a | 1.52 (1H, ddd, 12.0, 9.5, 3.0) | 33.2 | 2.61 (1H, ddd, 13.5, 10.5, 3.5) | 45.7 |
| 6b | 3.11 (1H, m) | | 2.75 (1H, ddd, 13.5, 10.5, 3.5) | |
| 7 | | 64.2 | | 202.9 |
| 8 | | 146.9 | | 138.3 |
| 9 | 7.62 (1H, d, 7.5) | 123.6 | 7.31 (1H, dd, 7.5, 1.5) | 128.7 |
| 10 | 7.25 (1H, td, 7.5, 1.5) | 127.0 | 7.25 (1H, td, 7.5, 1.5) | 126.3 |
| 11 | 7.33 (1H, td, 7.5, 1.5) | 128.4 | 7.51 (1H, td, 7.5, 1.5) | 132.4 |
| 12 | 7.50 (1H, d, 7.5) | 121.5 | 7.65 (1H, dd, 7.5, 1.5) | 123.8 |
| 13 | | 154.1 | | 141.9 |
| 14a | 1.85 (1H, m) | 19.3 | 1.53 (1H, ddt, 13.5, 5.0, 2.5) | 23.2 |
| 14b | 2.64 (1H, m) | | 1.88 (1H, m) | |
| 15a | 5.83 (1H, dd, 3.5, 1.5) | 124.2 | 1.11 (1H, td, 13.5, 5.0) | 33.5 |
| 15b | | | 1.72 (1H, m) | |
| 16 | | 81.0 | 5.05 (1H, dd, 4.5, 2.0) | 91.9 |
| 17a | | | 1.88 (1H, m) | 27.8 |
| 17b | | | 2.93 (1H, m) | |
| 18 | 1.10 (3H, d, 6.5) | 11.2 | 0.90 (3H, t, 7.5) | 7.7 |
| 19a | 2.74 (1H, m) | 43.6 | 1.21 (1H, m) | 31.9 |
| 19b | | | 1.85 (1H, m) | |
| 20 | | 135.7 | | 37.6 |
| 21 | 3.33 (1H, br s)[c] | 69.1 | 2.51 (1H, br s) | 75.9 |
| $CO_2Me$ | | 173.4 | | |
| $CO_2Me$ | 3.84 (3H, s) | 52.7 | | |
| OH | 4.87 (1H, br s) | | | |
| OMe | | | 3.47 (3H, br s) | 54.7 |

[a] 500 MHz, acetone-$d_6$.
[b] 125 MHz, acetone-$d_6$.
[c] Overlapped.

## 3. Results and discussion

### 3.1. Structure elucidation of the compounds

Bousangine A (**1**) was obtained as an optically active white solid, [α]20 D + 20.7 (*c* 0.16, $CH_3OH$). Its molecular formula $C_{20}H_{22}N_2O_3$ was established by HRESIMS ion at *m/z* 339.1708 ($[M + H]^+$, calcd for $C_{20}H_{22}N_2O_3$, 339.1703), corresponding to eleven degrees of unsaturation. IR absorptions implied the presence of ester carbonyl (1737 $cm^{-1}$) and hydroxyl (3433 $cm^{-1}$) functions. $^{13}C$ and DEPT spectroscopy suggested that **1** possessed 20 carbons including two methyls, four methylenes, seven methines including five $sp^2$ ones, and seven quaternary carbons including five $sp^2$ ones. Among them, the characteristic indolenine moiety, an ester carbonyl, and a trisubstituted double bond accounted for eight out of 11 degrees of unsaturation, the remaining three degrees of unsaturation indicated the presence of a tricyclic ring system in **1** (Fig. 1).

Four partial structural units **a** (C-5 to C-6), **b** (C-14 to C-3 and C-15), **c** (C-9 to C-12), and **d** (C-18 to C-19), drawn with bold bonds in Fig. 2, were deduced from the analysis of the 2D NMR spectra including HSQC and $^1H$–$^1H$ COSY. HMBC correlations established the connectivities between the partial structures and the quaternary carbon, as well as nitrogen atoms. In the HMBC spectrum, correlations of H-3a ($\delta_H$ 3.04) with C-5 ($\delta_C$ 47.2) and C-21 ($\delta_C$ 69.1) suggested that C-3, C-5, and C-21 were connected to each other through a nitrogen atom. HMBC

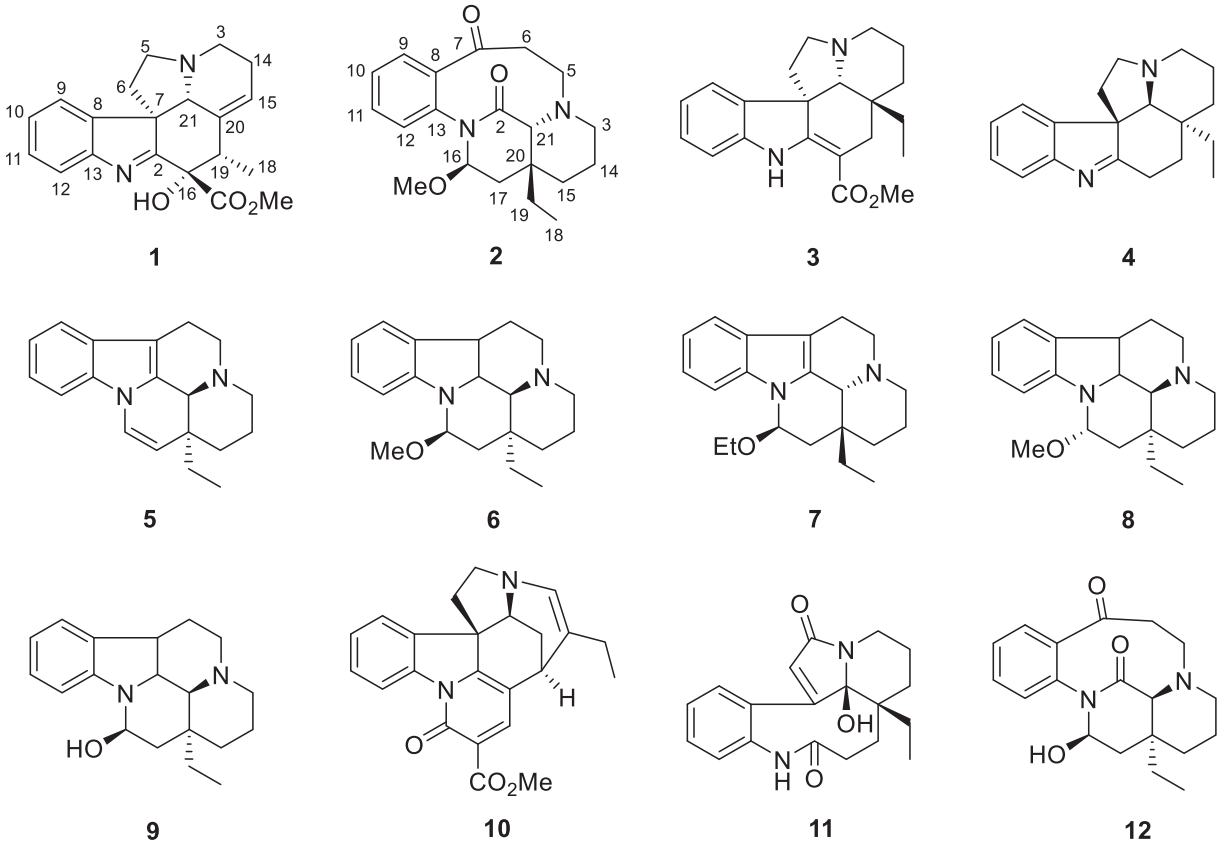


**Fig. 1.** Structures of compounds **1–12**.

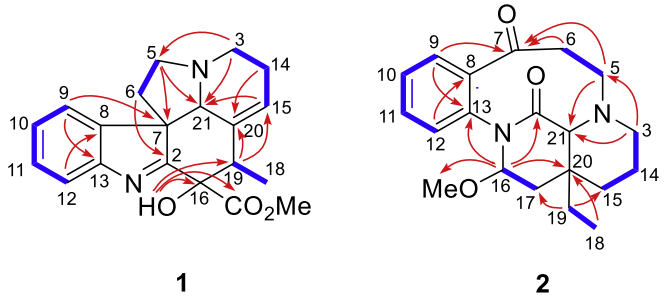


**Fig. 2.** Key HMBC (arrow) and $^{1}H-^{1}H$ COSY (bold) correlations of compounds **1** and **2**.

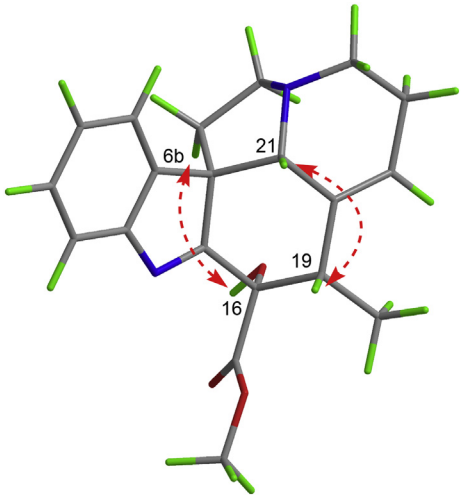


**Fig. 3.** Key ROESY correlations of compound **1**.

correlations of H-9 ($\delta_H$ 7.62) and H-5b ($\delta_H$ 3.33) to C-7 ($\delta_C$ 64.2), and of H-6b ($\delta_H$ 3.11) to C-2 ($\delta_C$ 182.2) suggested the linkage of indolenine moiety and fragment **a** via C-7. HMBC cross-peaks of H-19 ($\delta_H$ 2.74) to C-20 ($\delta_C$ 135.7) and C-15 ($\delta_C$ 124.2), and of H-15 ($\delta_H$ 5.83) to C-21 ($\delta_C$ 69.1) implied that C-15, C-19, and C-21 were connected to C-20, which also established the connectivities between fragments **b** and **d**. HMBC cross-peaks of OH to C-16 ($\delta_C$ 81.0), C-19 ($\delta_C$ 43.6) and the ester carbonyl carbon ($\delta_C$ 173.4) implied the linkage of hydroxyl, ester carbonyl carbon, and C-19 through the oxygenated quaternary carbon (C-16). Though key HMBC correlations of H-19 and OH with C-2 were not observed, the connectivity between the two quaternary atoms, C-2 and C-16, was established by the remaining one degree of unsaturation. Thus, the planar structure of **1** featured an unprecedented pentacyclic ring system was finally established as shown in Fig. 2.

The relative configuration of **1** was deduced from the analysis of its ROESY spectra (Fig. 3). The ROESY correlation of H-19/H-21 indicated that both protons were co-facial and were assigned arbitrarily as *β*-oriented. Meanwhile, the observation of weak correlation of H-6b/16-OH revealed that 16-OH might be α-oriented. Therefore, the relative configurations of **1** was assigned as (7*S**,16*S**,19*S**,21*R**)-**1** or (7*S**,16*R**,19*S**,21*R**)-**1**. To confirm the above elucidation, the $^{13}C$ NMR data were computed by using DFT studies at the B3LYP/6–311 + G(2d,p) level for the two selected isomers, (7*S*,16*S*,19*S*,21*R*)-**1** and (7*S*,16*R*,19*S*,21*R*)-**1** [15]. The observed experimental $^{13}C$ NMR data matched up to the calculated data for the isomer (7*S*,16*S*,19*S*,21*R*)-**1**, thus indicating a 16*S** configuration (Table S1).

The absolute configuration of **1** was finally determined by time-dependent density functional theory (TDDFT) ECD calculations. The calculation for two possible enantiomers (7*S*,16*S*,19*S*,21*R*)-**1** and (7*R*,16*R*,19*R*,21*S*)-**1** were performed, and the results demonstrated that

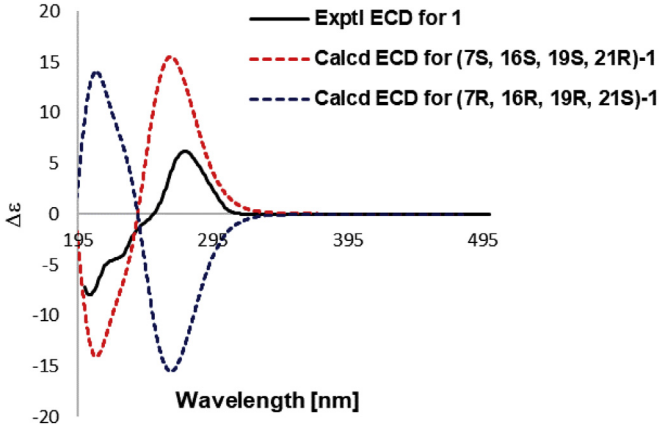


**Fig. 4.** Experimental and calculated ECD of **1**.

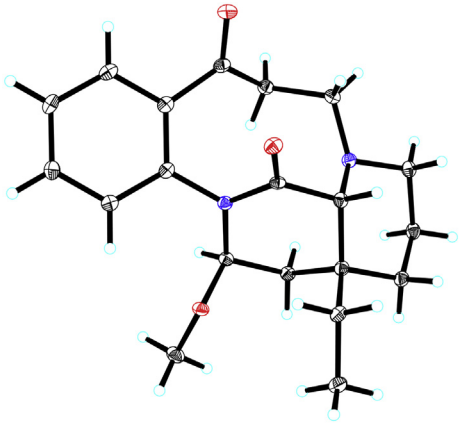

**Fig. 5.** X-ray crystal structure of **2**.

the calculated ECD curve for (7*S*,16*S*,19*S*,21*R*)-**1** matched well with its experimental ECD spectrum (Fig. 4), which finally established the absolute configuration of **1**.

A plausible biosynthetic pathway for the production of **1** was proposed in Scheme 1. The biogenetic precursor might be originated from (+)-vincadifformine which underwent Wagner-Meerwein rearrangement to generate key intermediate **ii**. Further oxidation and Bayer-Villiger rearrangement could afford intermediate **iii**. The subsequent decarboxylation yielded intermediate **iv**, which further transformed to **v** via an intramolecular Michael addition reaction. Compound **1** could be finally obtained under further dehydration and oxidation of **v**.

Bousangine B (**2**) was obtained as an optically active colorless solid, [α]20 D − 36.2 (*c* 0.11, $CH_3OH$). Its molecular formula, $C_{20}H_{26}N_2O_3$, was established by HRESIMS analysis (found: *m/z* 365.1846 $[M + Na]^+$; calcd for $C_{20}H_{26}N_2O_3Na$, 365.1836), corresponding to nine degrees of unsaturation. IR absorptions implied the presence of carbonyl (1735 $cm^{-1}$) function.

Detailed analysis of its NMR spectra indicated that **2** was an eburnean-type alkaloid and had a high similarity with that of melohenine B [16]. The major difference was the presence of an additional methyl ($\delta_H$ 3.47; $\delta_C$ 54.7). The key HMBC correlations of H-16 ($\delta_H$ 5.05) to the methyl ($\delta_C$ 54.7) indicated that the methyl was located at C-16 (Fig. 2). 2D NMR spectra (HSQC, HMBC, and $^1H-^1H$ COSY) confirmed the other parts of the structure were same as those of melohenine B. The ROESY correlations of H-21/$CH_2$–19 established these protons were co-facial and assigned arbitrarily as *β*-oriented. Meanwhile, the coupling constant of $J_{H\text{-}16/H\text{-}17a}$ (4.5 Hz) and $J_{H\text{-}16/H\text{-}17b}$ demonstrated that H-16 took α-orientation. The relative and absolute configurations of **2** was finally established by X-ray diffraction analysis with Flack parameter 0.02 [4] (Fig. 5) [17].

### 3.2. Cytotoxic activity

Two new compounds were evaluated for their antiproliferative activity against five human cancer cell lines: KB, KB-VIN, A549, MCF-7, and MDA-MB-231 using the sulforhodamine B (SRB) method with vincristine (VIN) and paclitaxel (PXL) as positive controls. Unfortunately, both of them was inactive with $IC_{50}$ > 10 μM.

## 4. Concluding remarks

In this investigation, two novel monoterpenoid indole alkaloids (**1–2**) and 10 known substances (**3 − 12**) were isolated from the twigs and leaves of *B. angustifolia*. Bousangine A (**1**) possessed an unprecedented rearrangement pentacyclic skeleton derived from aspidosperma- type alkaloids with C-17 degradation, while bousangine B (**2**) was a new eburnean-type MIAs. Their structures including absolute configurations were established by a combination of HRMS, NMR, ECD calculation, and X-ray diffraction analysis. Their antiproliferative activity were also evaluated and none of them was active.

## Declaration of Competing Interest

Authors declare that there is no conflict of interest.

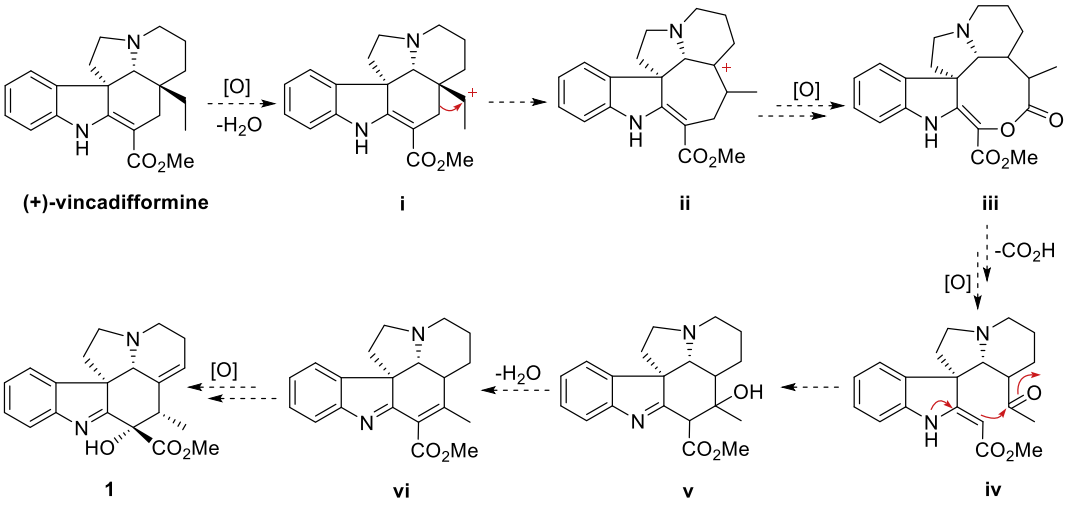


**Scheme 1.** Plausible biosynthetic pathway for compound **1**.

## Acknowledgements

This work was financially supported by the NSFC (81874295), Yunnan Applied Basic Research Projects (2018FA049), Top Young Talent of the Ten Thousand Talents Program of Yunnan (to Y. Zhang), and the Young Academic and Technical Leader Raising Foundation of Yunnan (to Y. Zhang).

## Appendix A. Supplementary data

Supplementary data to this article can be found online at https://doi.org/10.1016/j.fitote.2020.104491.

## References

[1] P.M. Dewick, Alkaloids, Medicinal Natural Product: A Biosynthetic Approach, John Wiley & Sons ltd, Chichester, 2002, pp. 340–341.
[2] B.T. Li, J.M. Leeuwenberg, D.J. Middleton, Flora of China, 16 (1995), p. 150.
[3] Y.H. Fu, S.L. Li, S.F. Li, H.P. He, Y.T. Di, Y. Zhang, X.J. Hao, Fitoterapia. 98 (2014) 45–52.
[4] Y.H. Fu, Y.T. Di, H.P. He, S.L. Li, Y. Zhang, X.J. Hao, J. Nat. Prod. 77 (2014) 57–62.
[5] Y.H. Fu, H.P. He, Y.T. Di, S.L. Li, Y. Zhang, X.J. Hao, Tetrahedron Lett. 53 (2012) 3642–3646.
[6] Y.L. Wang, C.R. Guo, Y. Mu, Y.L. Lin, Tetrahedron Lett. 60 (2019) 151042.
[7] Y. Zhang, M. Goto, A. Oda, P.L. Hsu, L.L. Guo, Y.H. Fu, X.J. Hao, Molecules 24 (2019) 1256.
[8] I. Chazelet, F. Batchily, H. Mehri, M. Plat, Ann. Pharm. Fr. 44 (1987) 355–562.
[9] P. Pfaffli, H. Hauth, Helv. Chim. Acta. 61 (1978) 1682–1695.
[10] R. Atta, K. Zaman, S. Perveen, R. Habib, A. Muzaffar, M.I. Choudhary, A. Pervin, Phytochemistry 30 (1991) 1285–1293.
[11] S. Baassou, H. Mehri, M. Plat, Ann. Pharm. Fr. 45 (1987) 49–56.
[12] Y.Q. Wu, M. Kitajima, N. Kogure, Y.S. Wang, R.P. Zhang, H. Takayama, Chem. Pharm. Bull. 58 (2010) 961–963.
[13] C.Y. Gan, Y.Y. Low, T. Etoh, M. Hayashi, K. Komiyama, T.S. Kam, J. Nat. Prod. 72 (2009) 2098–2103.
[14] J. Yang, J. Fu, X. Liu, Z.H. Jiang, G.Y. Zhu, Fitoterapia 124 (2018) 73–79.
[15] D.A. Forsyth, A.B. Sebag, J. Am. Chem. Soc. 119 (1997) 9483–9494.
[16] T. Feng, X.H. Cai, Y. Li, Y.Y. Wang, Y.P. Liu, M.J. Xie, X.D. Luo, Org. Lett. 11 (2009) 4834–4837.
[17] H.D. Flack, G. Bernardinelli, Chirality 20 (2008) 681–690.